A bilateral comparison of particle number concentration standards via calibration of an optical particle counter for number concentration up to ~1000 cm^{-3}

Thomas Y. Wu[a,*], Yoshiko Murashima[b], Hiromu Sakurai [b], Kenjiro Iida [b]

[a] *National Metrology Centre, A*STAR, 2 Fusionopolis Way, #08-05, Innovis, Singapore*

[b] *National Institute of Advanced Industrial Science and Technology (AIST), 1-1-1 Umezono, Tsukuba, Ibaraki, 305-8563, Japan*

*Corresponding author. *Email:* yongusa@qq.com

Abstract

The first bilateral comparison of particle number concentration (PNC) standards via calibrating the counting efficiency (CE) of an optical particle counter (OPC) at high concentration of 1000 cm^{-3} is reported. An OPC (GRIMM 11-D) has been used as the transfer standard between NMC and NMIJ, with its CE being calibrated using monodisperse polystyrene latex (PSL) particles around 0.3 µm by the Faraday Cup Aerosol Electrometers (FCAE) of both metrology institutes. The CE of the OPC has been evaluated for a series of increasing concentrations to determine the highest concentration level which is free from coincidence loss. The OPC was also calibrated at 0.5 µm using an inkjet aerosol generator (IAG) and FCAE to compare its CE at different concentration levels. We have analysed the CE's stability at decreasing concentration levels from 1228 to 0.5 cm^{-3} to derive the evidence for the equivalence of CE at different concentration levels. The CE values of the OPC around 0.3 and 0.5 µm measured by two institutes have agreement within 1.5% (normalized error $E_n < 1$), which can serve as evidence of the equivalence of the PNC standards of both metrology institutes for concentrations up to 1000 cm^{-3}. The measurement setup, comparison results and uncertainty analysis for the OPC calibration have been presented.

Keywords: aerosol metrology, optical particle counter, counting efficiency, coincidence error, measurement uncertainty, aerosol electrometer, inkjet aerosol generator

1. Introduction

The aerosol particle counters have been widely used for aerosol particle size distribution analysis and concentration measurement in clean room, indoor air, ambient air or filtration testing [1–8]. In a single-particle optical particle counter (OPC), the scattered light at different angles is collected, and the light intensity is determined by the particle size, shape, refractive index, and scattering angle [9,10,19,20,11–18]. Particles are classified into multiple size channels according to the scattered light signal levels and countings are made for each channel. Various techniques have been used to calibrate an OPC to ensure high accuracy and traceability in aerosol particle size and number concentration measurement [21–29]. Other types of instruments for measuring particle number concentration include condensation particle counters (CPC), scanning mobility particle sizer (SMPS), aerodynamic particle sizer (APS) and electrical low pressure impactor (ELPI).

Currently the aerosol particle counting measurement instruments are traceable to Faraday Cup Aerosol Electrometer (FCAE) or inkjet aerosol generator (IAG) [30–36]. The particle concentration measurement made by FCAE is traceable to electrical low current primary standard. The monodisperse particle generation rate of IAG can be controlled precisely with traceability to frequency counter, which can serve as a particle number concentration (PNC) standard. International comparison of PNC standards between national metrology institutes (NMI) is very important to establish the equivalence of such metrology standards across different countries. Smaller deviations between NMIs in such comparisons are also needed to validate the lower uncertainty of PNC standards.

Till now, only a few inter-NMI comparisons have been conducted for particle concentration measurement. The first comparison was performed using combustion aerosol particles from 50 to 170 nm using CPC, SMPS and ELPI as measurement instrument, with concentrations at 1000 to 1000000 cm^{-3} [37]. The comparison of concentration measurement via CPC counting shows agreement within 5%. Another comparison using CPC was conducted using soot and silver particles at concentrations range 100 to 20000 cm^{-3} and particle sizes from 13 to 100 nm, with agreement within 10% between the laboratories [38]. A bilateral comparison was performed by calibrating a single CPC in a wide particle size range from 10 nm to 1 μm and concentration at 6, 3200 and 7850 cm^{-3} , with correction applied to remove the concentration effect on the CPC's counting efficiency (CE) [34]. The CE's agreement is within ~2% for the overlapping particle sizes between the two NMIs. A comprehensive inter-NMI comparison of FCAE was done for particle sizes from 20 to 200 nm in the concentration range 1000 to 17000 cm^{-3} , with an agreement within 6.5% for counting at lower concentrations at 1000 cm^{-3} (except for one laboratory) [39].

The OPCs are portable instruments for particle count measurement with good repeatability and accuracy, thus they can serve as a transfer standard to compare the performance of PNC standards of various countries [34,40–42]. The first inter-NMI comparison of OPC's CE for low concentration range (up to 2 cm^{-3}) between the metrology institutes of Japan, Denmark and Switzerland has been reported in [43]. Polystyrene latex (PSL) particles with size at around 0.3, 0.5, 1 and 5 μm have been used to compare the CE of three models of OPC for low concentrations around 0.06 cm^{-3} and 0.6 – 2 cm^{-3} . This comparison was done at different concentration levels for two OPC models, and the results show an agreement within 7% to demonstrate the equivalence of the PNC standards in these three NMIs.

For aerosol concentration measurement of indoor air or ambient air, the CE of OPC needs to be calibrated with traceability at particle concentration level much higher than 2 cm^{-3}. Comparison of OPC's CE between NMIs for higher concentration around 1000 cm^{-3} has not been reported in literature. In this paper, the first inter-NMI comparison on the CE of OPC using particle size around 0.3 and 0.5 μm at higher concentration (up to ~1000 cm^{-3}) is reported. An OPC (GRIMM 11-D) with 31 size channels has been used as the transfer standard. The OPC's CE was calibrated using PSL particles around 0.3 μm at concentration of ~1000 cm^{-3} by the FCAE of both institutes. The OPC's CE was also calibrated at 0.5 μm using IAG of NMIJ at concentration around 0.5 cm^{-3} and the FCAE of NMC at concentration of ~1000 cm^{-3}. Although the CE was compared at different concentration levels at 0.5 μm, the CE only shows small variation (<1.6%) at decreasing concentration levels from 1228 to 0.5 cm^{-3}, which basically comes from measurement noise. With the CE's stability demonstrated at decreasing concentration levels and E_n <1, this comparison has given strong evidence for the equivalence of PNC standards at 0.5 μm of both institutes.

The measurement setup at the two NMIs and comparison results for the CE are presented. The detailed uncertainty analysis for OPC calibration using the PNC standard of NMC is presented for the first time. The updated uncertainty budgets for OPC calibration using the PNC standard of NMIJ have been reported for the latest setup. These uncertainty analysis can serve as useful references to other NMI and calibration laboratories in the area of aerosol particle metrology.

The CE of the OPC (around 0.3 μm) has been evaluated for a series of increasing concentrations to determine the highest particle concentration level which is not affected by the coincidence error of the OPC. This evaluation helps us to select a suitable particle concentration level for this comparison so that we don't need to consider the coincidence error effect on counting efficiency. We will also discuss the monodisperse particles generated for the calibration of OPC and compare their size distribution as measured by the OPC. This new comparison of OPC's CE at concentration up to 1000 cm^{-3} shows that an agreement within 1.5% has been achieved for the PNC of the two NMIs, which is better than previous international comparisons. This comparison is important to ensure that our PNC standards can provide accurate reference values for OPC calibration and dissemination down the traceability chain to other industrial laboratories for clean room control, air quality monitoring, or filtration testing.

2. Measurement systems of NMC and NMIJ

2.1. Measurement setup at NMC

At NMC, a primary aerosol electrometer is used to calibrate the OPC using PSL particles, which are generated by a TOPAS atomiser aerosol generator (ATM 220). An aerosol charge neutraliser is used to apply an equilibrium charge distribution to the aerosols produced by the aerosol atomiser [44–47]. A differential mobility analyzer (DMA) is used as an electrostatic size classifier to select particles with a diameter centred at the mean diameter size [48–50]. The sheath air flowrate for DMA is set as Q_{sh}=10 L/min. The total particle flowrate from the aerosol generator is 2.2 L/min. A flow splitter is used to split the particle flow to OPC and aerosol electrometer (GRIMM 5.705). The particle sample flowrate is 1.2 L/min for OPC (GRIMM 11-D) and 1 L/min for aerosol electrometer, respectively. The particle concentration is around 1000 cm^{-3}. Fig. 1 shows the diagram of the measurement setup at NMC.

The aerosol sample flow is drawn through a particle filter inside a metal cage in the aerosol electrometer to produce a low electrical current (ΔI) in femto-ampere range. The particle number concentration, C, is a function of the ion current (ΔI) as shown below

$$C = \frac{\Delta I}{z\, e\, Q} \qquad (1)$$

where z is the average number of charges on aerosol particles, e is the elementary charge (1.602 × 10^{-19} C) and Q is the volumetric flow rate into the aerosol electrometer. The particles flown into the aerosol electrometer contain single-charged and multiple-charged particles, with corresponding charging probabilities [47]. The average number of charges on aerosol particles (z) can be evaluated using the charging probabilities and the size distribution of the particles entering the DMA [36]. The ion current is measured accurately to calculate the aerosol particle number concentration based on the sample flow rate, size distribution and the charging probabilities of the aerosol particles [39,51–55]. The aerosol electrometer of NMC is traceable to the DC low current standard of Physikalisch-Technische Bundesanstalt (PTB).

The OPC's CE is derived from the ratio of the particle concentration reading by OPC (C_o) and the particle concentration reading by the aerosol electrometer (C_a), as shown below

$$\text{CE} = \frac{C_o}{C_a} \qquad (2)$$

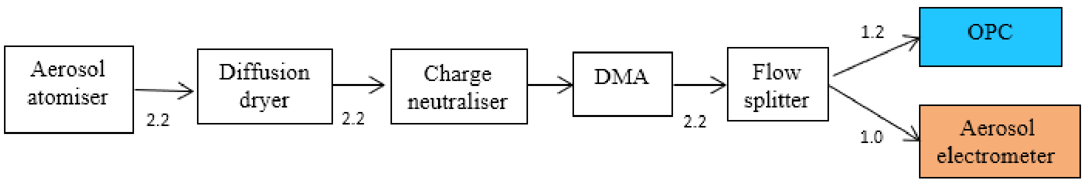

Fig. 1 Measurement setup at NMC to calibrate the OPC's CE using a FCAE

2.2. Measurement uncertainty of NMC's PNC standard

The NMC's aerosol electrometer (GRIMM 5.705) has been calibrated by a low current standard of PTB using the charging capacitor method from 5 to 1000 fA [56]. The calibration data using reference currents is used to derive a current response factor to make correction of the current measured by the aerosol electrometer for particle concentration around 1000 cm^{-3}. The relative standard uncertainty of the response factor for low current measurement is estimated to be u_{ref} = 0.32 %. There is random noise in the particle number concentration measurement made by the aerosol electrometer, which is due to the ion current measurement noise. The relative standard uncertainty due to current measurement noise is estimated to be u_{ae} = 0.70 % (for ion current level at ~3 fA) based on electrometer's measurement data when measuring at particle concentration around 1000 cm^{-3}.

The aerosol electrometer's sampling flowrate has a relative standard uncertainty of u_f = 0.50% based on the calibration result. This uncertainty factor will directly contribute to the particle number concentration measured by the aerosol electrometer, which is derived using the total particle count for a given sample-volume (affected by the sampling flowrate).

There is particle concentration difference between the port 1 and port 2 outlets of the flow splitter. Experiments are conducted to evaluate this splitter bias effect by calibrating the CE of OPC at different splitter ports. The CEs of OPC using port 1 and port 2 show a relative error limit e_b = 0.57 % (worst case due to splitter bias). Thus the relative standard uncertainty due to splitter bias effect can be estimated as $u_b = e_b / \sqrt{3}$ = 0.33 % in the calibration of OPC, assuming a rectangular distribution [57].

The stability of aerosol particle concentration in the sample flow from the generator will affect the readings of OPC and aerosol electrometer, which contribute to the uncertainty in the measured CE. The relative standard uncertainty due to aerosol number concentration's fluctuation effect is estimated from the measured data to be $u_o = u_a$ = 0.20 % (u_o for the effect through the OPC, u_a for the effect through the aerosol electrometer, respectively).

Based on the actual measurement data, the relative standard uncertainty due to OPC measurement noise (u_{ns}) is estimated to be 0.29 % and 0.25 %, respectively, for particle size around 0.3 and 0.5 μm (for particle concentration around 1000 cm^{-3}). The repeatability of CE of OPC (u_r) is derived from the actual measurement data statistics as type A uncertainty [57], with values given in table 1. The uncertainty for the z (average number of charges on aerosol particles) is considered to be negligible.

These standard uncertainty components are combined using the equation below to yield the relative combined uncertainty for CE. The uncertainty budget details are shown in table 1.

$$u_{\mathrm{CE}} = \sqrt{u_{\mathrm{ae}}^2 + u_{\mathrm{ref}}^2 + u_{\mathrm{f}}^2 + u_{\mathrm{b}}^2 + u_{\mathrm{o}}^2 + u_{\mathrm{a}}^2 + u_{\mathrm{ns}}^2 + u_{\mathrm{r}}^2} \qquad (3)$$

The expanded uncertainty for CE (coverage factor k=2) is obtained as

$$U = 2\, u_{\mathrm{CE}}\, \mathrm{CE} \qquad (4)$$

Table 1. Uncertainty budget for calibration of CE of OPC at NMC with PSL particle size around 0.3 and 0.5 µm (with flowrate of 1.2 L/min and particle concentration at ~1000 cm^{-3}).

Uncertainty component	**Type**	**Relative standard uncertainty (around 0.3 µm)**	**Relative standard uncertainty (around 0.5 µm)**
Current measurement response factor of aerosol electrometer, u_{ref}	B	0.32%	0.32%
Aerosol electrometer current measurement noise, u_{ae}	B	0.70%	0.70%
Aerosol electrometer's sampling flowrate uncertainty, u_f	B	0.50%	0.50%
Flow splitter bias, u_b	B	0.33%	0.33%
Aerosol concentration fluctuation effect on OPC, u_o	B	0.20%	0.20%
Aerosol concentration fluctuation effect on aerosol electrometer, u_a	B	0.20%	0.20%
OPC measurement noise, u_{ns}	B	0.29%	0.25%
Repeatability of OPC's CE, u_r	A	0.57%	0.67%
Relative combined standard uncertainty for CE		**1.20%**	**1.24%**
CE of OPC		0.976	0.992
Expanded uncertainty for the CE (*k*=2)		0.024	0.025

2.3. Measurement setup at NMIJ using a FCAE

Fig. 2 shows the diagram of the measurement setup at NMIJ which is based on FCAE. The OPC (GRIMM 11-D) is calibrated using a FCAE [34,52] using PSL particles of mean size at 0.3 µm. The calibration setup detail has been given in [34]. For this comparison exercise, the sheath and aerosol flowrates of DMA are set as Q_{sh}=7.5 L/min and 1.5 L/min, respectively, and both the FCAE and OPC sample flowrates are 1.2 L/min. A flow splitter is used to split the particle flow to FCAE and OPC. PSL particles were aerosolized with a TSI 3480 Electrospray Aerosol Generator equipped with an Am-241 charge conditioner (not shown in the figure), followed by another Am-241 charge conditioner. The particle concentration was adjusted to ~1000 cm^{-3} with the diluter between the second charge conditioner and the DMA.

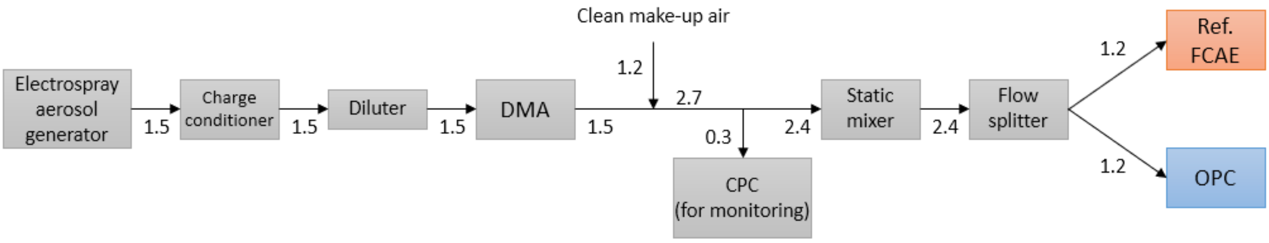

Fig.2 Measurement setup at NMIJ to calibrate the OPC's CE using a Faraday cup aerosol electrometer (FCAE).

The updated uncertainty budget for calibration of OPC at NMIJ using FCAE is shown in Table 2. The relative standard uncertainty for current measurement by the FCAE is a combination of the relative standard uncertainty reported in [52] (0.354%) and a relative standard uncertainty for annual variability (0.211%) that was evaluated after the publication of [52]. The flow splitter bias and its uncertainty were determined by the method described in ISO 27891:2015 [58]. The repeatability of the OPC's CE was evaluated as a type A uncertainty during the measurement at concentrations of ~1000 cm^{-3} in this study with repetitions greater than 15. The average number of charges on 0.3 μm PSL particles thus generated was 1.001 [36,58] and its uncertainty was negligible compared to the other measurement uncertainties. The expanded uncertainty is estimated as 0.017 (k = 2) for calibration of the CE using FCAE with PSL particle size at 0.3 μm.

Table 2. Uncertainty budget for calibration of OPC at NMIJ using a FCAE, using PSL particle size at 0.3 μm with flowrate of 1.2 L/min and particle concentration at 1000 cm^{-3}

Uncertainty Component	**Type**	**Rel. std. uncertainty**
Current measurement	B	0.41 %
Flow rate measurement	B	0.22 %
Flow splitter bias	B	0.24 %
Repeatability	A	0.72 %
Relative combined standard uncertainty		0.89 %
CE of OPC		0.966
Expanded uncertainty of the CE (*k* = 2)		**0.017**

2.4. Measurement setup at NMIJ using an IAG

For particle size at 0.5 μm, the OPC is calibrated using an IAG with lactose monohydrate (LM) particles. The IAG generates monodisperse LM test particles at a precisely controlled rate [59–61] . The rate of particle number being generated by the IAG was L = 10.00 s^{-1} with an expanded uncertainty of 0.052 s^{-1} (k = 2). The particle concentration generated is given by $C_{\mathrm{primary}} = L/Q$ = 0.5034 cm^{-3}, where Q is the measured sample flowrate of the OPC (11-D). Fig. 3 shows the schematic description of the calibration setup.

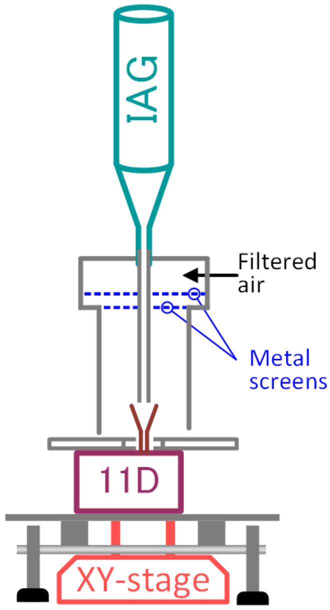

Fig. 3 Measurement setup at NMIJ to calibrate the OPC's CE using an inkjet aerosol generator (IAG)

The IAG-based calibration method simulates the sampling of uniformly mixed aerosol particles by delivering test particles at various places over the inlet plane of the sampling probe [59,60]. The OPC (GRIMM 11-D) was placed on a table with a motorized XY-stage which was programmed to bring the tip of the IAG-exit tube to specific points within the inlet plane of the sampling probe [60]. A sampling probe with a tapered inlet has been designed for GRIMM 11-D. The inlet and outlet diameter of the probe were 30 mm and 3 mm, respectively. The full angle of the tapered section is 40 degrees. The sampling probe was inserted into the inlet of the OPC, which is a quick fitting for a tube with outer diameter of 4 mm. Although the best efforts have been made in the IAG-based measurement to deliver LM particles uniformly over the inlet plane of sampling probe, the delivery method may not be sufficient in simulating the sampling of uniformly mixed aerosols.

The updated measurement uncertainty budget for OPC calibration using the IAG system (shown in Fig 3) for particle size around 0.5 μm is given in Table 3. The relative particle count rate uncertainty due to the unknown aerosol velocity profile over the inlet plane of sampling probe is 0.20% (k=1). The relative standard uncertainty due to the particles potentially not sampled at the outer edge of sampling probe is estimated to be 0.19%. The particle generation rate of the IAG has a relative standard uncertainty of 0.26%. The measurement repeatability for the OPC calibration is 0.10% (type A uncertainty). The expanded measurement uncertainty of the OPC's CE using IAG system is estimated as 0.009 (k = 2). For more details on the uncertainty analysis in OPC calibration using IAG system, readers can refer to reference [60].

Table 3. Uncertainty budget for calibration of OPC at NMIJ using an IAG with LM particle size around 0.5 µm, with flowrate of 1.2 L/min and particle concentration at ~0.5 cm^{-3}

Uncertainty Component	**Type**	**Rel. std. uncertainty**
Particle count rate uncertainty due to unknown aerosol velocity profile over the inlet plane of sampling probe	B	0.20%
Particles potentially not sampled at the outer edge of sampling probe	B	0.19%
Sampling flowrate of the OPC	A	0.18%
Particle generation rate of the IAG	A	0.26%
Repeatability	A	0.10%
Relative combined standard uncertainty		0.43%
CE of OPC		0.980
Expanded uncertainty of the CE (*k* = 2)		**0.009**

3. Travelling standard for the comparison

3.1. Optical particle counter (OPC)

An OPC (GRIMM 11-D) has been used as the travelling standard for the comparison of the PNC standards. This OPC has the ability to count individual aerosol particles with good size resolution, and classifies particles into 31 logarithmic-scale equidistant channels spanning size range from 0.25 to 35.15 µm. It is based on wide-angle light scattering from particles flown through a measurement cell volume, with a sampling flowrate at 1.2 L/min.

This portable OPC is suitable to serve as the travelling standard due to its good stability and repeatability. Its CE is first calibrated by the NMIJ's PNC standard, followed by a calibration by NMC's standard.

3.2. Coincidence error of OPC

The CE of the OPC (at 0.3 µm) has been evaluated for a series of increasing concentrations to determine the highest particle concentration level which is not affected by the coincidence error of the OPC. This evaluation helps us to select a suitable particle concentration level for this comparison so that we don't need to consider the coincidence error effect on counting efficiency.

When the particle number concentration is too high inside the OPC's measurement cell, the detector may receive scattered signals from two and more particles in the beam direction, which means the coincidence errors will occur [22,23,62–68]. Such high concentrations will cause missed counts when new particles in the measurement cell are not counted during the dead time [69]. Another possibility is that multiple particles are classified as a larger particle (assigned into a bigger size channel), reducing the actual count for the correct size channel. High concentrations may change the scattered pulse width or shape, which may be invalidated and not counted by OPC firmware. The scattered signal baseline and noise floor may increase when the particle concentration is too high, which may lead to counting errors and reduction of CE in OPC [70,71]. All of these could lead to coincidence errors in OPC at higher particle concentrations.

Assuming a Poisson distribution for the particles present in the sensing volume, the fractional coincidence loss in OPC has been given in ISO 21501-4:2018 [24,28,64,72] as

$$LS = 1 - e^{-Q\, t_p\, C_{mx}} \qquad (5)$$

where Q is the flowrate, C_{mx} is the particle concentration, t_{p} is the sum of electrical processing time and time for a particle to pass through the sensing volume. However, this formula mainly considers the probability of multiple particle being in the sensing volume.

To study the coincidence error effect and stability of CE, the CE of OPC (GRIMM 11-D) was calibrated using a reference CPC with PSL particle size of 0.3 μm for particle concentrations from ~200 cm^{-3} to ~1500 cm^{-3} with fine steps (using the setup in Fig 2 with the FCAE replaced by a CPC). Fig. 4 shows that, for concentrations below 1245 cm^{-3}, the mean value for the CE of OPC (11-D) is derived as 0.976 and the relative deviations from this mean CE value are quite small (within 1.0%). Above the concentration of 1450 cm^{-3}, the CE of the OPC starts to decrease.

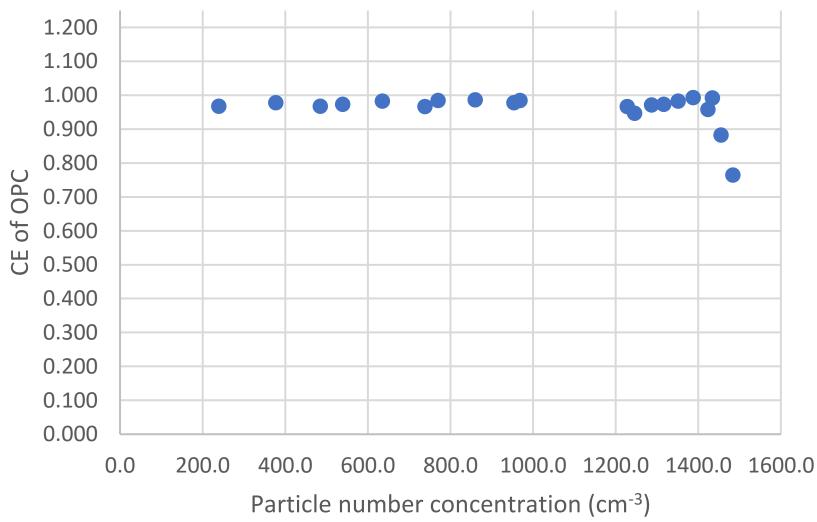

Fig. 4 The CE of OPC (GRIMM 11-D) vs. particle number concentration, calibrated using a CPC with PSL particle size of 0.3 μm, for particle number concentrations from ~200 to ~1500 cm^{-3}.

Table 4 shows the CE's relative deviation from the mean value of CE (0.976) for various concentration levels. At concentration of 1455 cm^{-3}, the CE's relative reduction is 9.6% from the mean CE value of 0.976. The CE's random deviations for concentration below 1245 cm^{-3} can be attributed to measurement noise effect (below 1.0%, which is smaller than the expanded measurement uncertainty of CE).

Table 4 CE's relative deviation from the mean value of CE for a range of concentration levels (mean value of CE is 0.976, derived from the CEs for particle concentrations below 1000 cm^{-3}), calibrated using a reference CPC with PSL particle size of 0.3 μm

Particle number concentration (cm^{-3})	CE of OPC (Grimm 11-D)	Rel. deviation from the mean CE value (0.976)
239.2	0.968	-0.8%
376.9	0.978	0.2%
484.3	0.967	-0.9%
538.6	0.974	-0.3%
635.2	0.983	0.7%
737.9	0.967	-1.0%
769.8	0.984	0.9%
859.7	0.986	1.0%
953.2	0.978	0.2%
968.1	0.985	0.9%
1228.1	0.967	-0.9%
1245.5	0.947	-3.0%
1286.8	0.971	-0.5%
1316.3	0.973	-0.3%
1351.2	0.983	0.7%
1387.5	0.993	1.7%
1423.5	0.958	-1.9%
1433.7	0.992	1.7%
1454.7	0.883	-9.6%
1483.9	0.765	-21.6%

The GRIMM 11-D's operation manual has specified the maximum particle concentration as 3000 cm^{-3} for full size range and recommended to use dilutor for concentration higher than 3000 cm^{-3} to avoid the coincidence error. The reason for reduction of CE of this 11-D unit at concentrations beyond 1450 cm^{-3} need to be investigated. The specific unit of 11-D used in this comparison maybe sensitive to particle concentration higher than 1450 cm^{-3}. In our future work, we will conduct further study to see whether the counting loss of OPC is due to higher noise floor, pulse distortion or coincidence. But the comparison result is not affected, since we have set the particle concentration to be ~1000 cm^{-3} (for FCAE based setup) which is free from coincidence loss. Particle concentration of lower than 1000 cm^{-3} is not used, since it will lead to higher noise in our FCAE (ion current below 3 fA) and higher uncertainties in calibration of OPC's CE.

For calibration of CE by the IAG using particle at 0.5 μm, the particle concentration is limited by the inkjet droplet generation rate to be 0.5 cm^{-3}, thus the coincidence error effect on CE can be ignored for the calibration setup using the IAG.

4. Particle size distribution measured by OPC

PSL particles have been used in the measurement by FCAE at NMC for the comparison at 0.5 μm, which is generated by TOPAS aerosol generator in Fig. 1. The certified mean diameter of PSL particle is 0.496 μm with relative standard uncertainty of 0.8% (0.004 μm, k=1), which has narrow range of variation in size. The PSL particle has shown a relative standard deviation of 3.8% (σ = 0.019 μm) in size distribution as measured by an SMPS, which includes the DMA's resolution effect and the particle size variability. Thus the PSL particles have a high degree of monodispersity.

LM particles generated by the IAG are evaporation residue of a solution. Solute and solvent of the solution are LM and ultrapure-water, respectively. Primary definition of the volume equivalent diameter (d_v) of the LM particle generated by the IAG is given by,

$$d_v = \left(\frac{6m}{\pi\rho} + d_r^3\right)^{1/3} \quad (6)$$

$$m = C_m \cdot m_d \quad (7)$$

where m is the particle mass (kg), m_d is the average mass of an inkjet droplet (kg), C_m is the mass concentration of the solute inside the inkjet solution (the mass of solute divided by the mass of solution). d_r is the diameter of the residue particle (m). ρ is the material density of the test particle (kg/m^3). Table 5 gives the values of the above parameters.

Table 5. Parameters for d_v calculation and their values for the inkjet LM droplet

Parameter	**Symbol**	**Value**
Average mass of an inkjet droplet	m_d	6.22×10^{-11} kg
Mass concentration of the solute (LM) inside the inkjet solution	C_m	2.56×10^{-6}
Material density of the LM	ρ	1540 kg/m^3
Diameter of the residue particle	d_r	0.128 μm

The value of C_m in equation (7) is calculated with d_v in equation (6) set to the targeted particle size (d_t) of 0.5 μm. The particle size channels of OPCs are calibrated with PSL spheres; therefore, the particles size measured by OPCs are defined as PSL equivalent optical diameter, d_o, and the measured mean value of d_o for the LM particle was 0.485 μm (derived from 10 measurements by an OPC with pulse height analyser). Table 6 shows the PSL equivalent optical diameter of the LM particles (d_o) and its relative deviation of -3.0% from the target particle diameter (d_t). The refractive index of LM is 1.53 [73] (lower than that of PSL which is 1.59 [74]), causing the PSL-equivalent optical diameter (d_o) to be slightly lower than the target diameter (d_t).

The CE of GRIMM 11-D were evaluated at particle size whose diameter value is sufficiently close to the targeted particle diameter (0.5 μm). The equivalent optical diameter of the LM particle has a relative standard deviation of 4.5% (σ = 0.022 μm), as measured by an OPC with pulse height analyser. The LM particles have a high degree of monodispersity.

Table 6. PSL equivalent optical diameter of the LM particle, d_o, generated by IAG

Target particle diameter, d_t, μm	**Volume equivalent diameter, d_v, μm**	**PSL equivalent optical diameter of LM particle, d_o**		
		Mean particle diameter, μm	**Relative standard deviation (measured by OPC)**	**relative deviation from d_t**
0.500	0.501	0.485	4.5% (σ = 0.022 μm)	-3.0%

We have studied the size distribution of PSL particles and LM particles around 0.5 μm, as measured by the OPC (GRIMM 11-D). The actual counts detected by the OPC (GRIMM 11-D) were found to be scattering in several size channels around the mean size of the PSL and LM particles, as shown in table 7. The particle counts quickly fall off as the channel size deviation from the mean particle size increases. The particle size distribution spreading is due to the sizing error and size resolution of the OPC. The percentage of total count in table 7 indicates that the size distribution of LM particles detected by the OPC is more concentrated in channel 4 (0.414 - 0.488 μm) and channel 5 (0.488 - 0.576 μm), as compared to that of PSL particles. For PSL particles, 85.4% particles are classified by the OPC into channel 4 and 5; whereas for LM particles, 97.9% particles are classified into channel 4 and 5. The classification by OPC for LM particles is more focused into channel 4 and 5. Compared to LM particles, the percentage of PSL particles being classified into channel 4 and 5 has reduced by 12.5%.

The light scattering depends on particle's shape and refractive index. Thus the OPC could show some differences in particle sizing for PSL and LM particles. Another potential reason for the discrepancy is the degree of particle dispersion in the test aerosols. OPC's sizing error and resolution limitation will also cause the difference in size distribution measured by 11-D [11,17,75].

If only the counts of channel 3 to 6 are included (covering the size range 0.352 – 0.679 μm), we will see an error of at least 3.4% for the CE measured using PSL particles and an error of only 0.1% for the CE measured by LM particles. This will lead to some deviation in the comparison of CE. Therefore, for the calculation of the CE of OPC, the particle counts of all channels of GRIMM 11-D have been summed up to avoid the missed counts due to OPC's size setting error and resolution limitation.

Table 7 Particle size distribution spreading as measured by OPC (GRIMM 11-D) for PSL and LM particles around 0.5 μm, due to the sizing error and size resolution of the OPC

OPC Channel Number		**1**	**2**	**3**	**4**	**5**	**6**	**7**	**8**
Particle size range, μm		0.253-0.298	0.298-0.352	0.352-0.414	0.414-0.488	0.488-0.576	0.576-0.679	0.679-0.800	0.800-0.943
PSL particle	particle count, cm^{-3}	8.3	20.0	54.4	620.7	254.4	60.5	5.8	1.1
	percentage of total counts	0.8%	1.9%	5.3%	60.6%	24.8%	5.9%	0.6%	0.1%
LM particle	particle count, cm^{-3}	0.0003	0.0001	0.0004	0.2759	0.2075	0.0093	0.0093	0.0000
	percentage of total counts	0.1%	0.0%	0.1%	55.9%	42.0%	1.9%	0.0%	0.0%

5. Comparison results and analysis

5.1. Comparison of CE

For comparison around 0.3 μm, the particle concentration is ~1084 cm^{-3} for the NMC's setup and ~1000 cm^{-3} for the NMIJ's setup based on FCAE. The difference of the CE of GRIMM 11-D measured by NMC and NMIJ is $\Delta_1 = CE_1 - CE_2$ =0.010, with normalised error E_n =0.3 [76], where E_n is derived as

$$E_\mathrm{n} = \frac{|CE_1 - CE_2|}{\sqrt{U_1^2 + U_2^2}} \qquad (7)$$

where U_1 and U_2 being the CE's expanded uncertainty using PNC standard of NMC and NMIJ, respectively.

The comparison results are given in Table 8 and Fig. 5. The reported CE of OPC from NMIJ using FCAE (for particle size at 0.3 μm) is an average of the measurements made in two separate days.

Table 8 Comparison result of the CE of OPC (GRIMM 11-D) for particle size around 0.3 μm

CE of OPC (by NMC), CE_1	expanded uncertainty for CE_1, U_1	CE of OPC (by NMIJ) , CE_2	expanded uncertainty for CE_2, U_2	deviation in CE (CE_1 -CE_2)	E_n
0.976	0.024	0.966	0.017	0.010	0.3

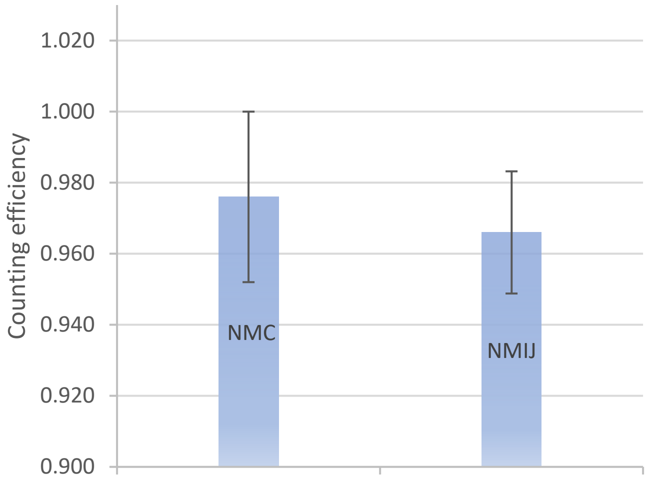

Fig. 5 Comparison result of the CE of OPC (GRIMM 11-D) for particle size around 0.3 μm, with error bar indicating the expanded uncertainty for the CE.

For comparison around 0.5 μm, the particle concentration is ~1020 cm^{-3} for the NMC's aerosol electrometer and ~0.5 cm^{-3} for the NMIJ's IAG-based setup. The difference of the CE of GRIMM 11-D measured by NMC and NMIJ is $\Delta_2 = CE_1 - CE_2 = 0.012$, with $E_n = 0.5$. The results are given in Table 9 and Fig. 6.

Table 9 Comparison result of the CE of OPC (GRIMM 11-D) for particle size around 0.5 μm

CE of OPC (by NMC), CE_1	expanded uncertainty for CE_1, U_1	CE of OPC (by NMIJ), CE_2	expanded uncertainty for CE_2, U_2	deviation in CE (CE_1 - CE_2)	E_n
0.992	0.025	0.980	0.009	0.012	0.5

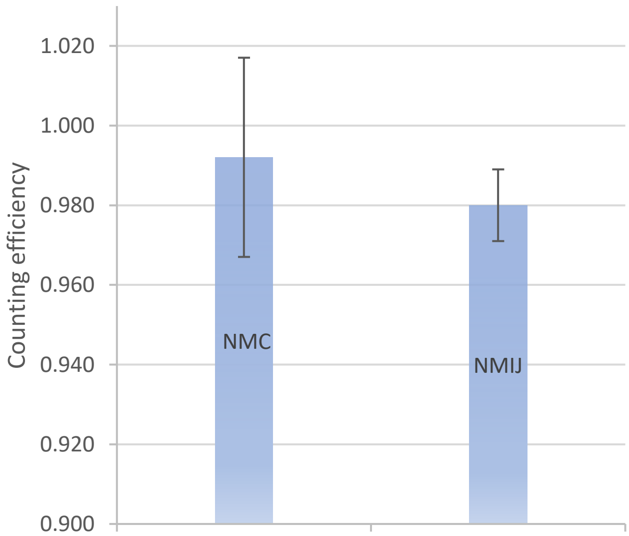

Fig. 6 Comparison result of the CE of OPC (GRIMM 11-D) for particle size around 0.5 μm, with error bar indicating the expanded uncertainty for the CE.

5.2. Discussion

The normalised error (E_n) for the comparison of OPC's CE around 0.3 μm is below 1, showing that the FCAE-based primary PNC standards of NMC and NMIJ are equivalent for high particle concentrations around 1000 cm^{-3} at particle size around 0.3 μm.

The coincidence error for GRIMM 11-D is assumed to be negligible for concentration up to 1000 cm^{-3}, since the relative deviation of CE from the mean CE value of 0.976 (in table 4) are all below 1.0% for concentration range up to 1228 cm^{-3}. Table 4 shows very small variations in the CE when particle concentration reduces from 1228 to 239 cm^{-3}. Based on the manufacturer test data, the CE of 11-D is 0.990 at concentration of 66 cm^{-3} (at 0.5 μm) and 0.992 at concentration of 79 cm^{-3} (at 0.3 μm). The CE of 11-D is 0.980 at concentration of 0.5 cm^{-3} which is measured by the IAG-based setup (at 0.5 μm). The CE's random fluctuations for various concentrations below 1228 cm^{-3} can be considered as measurement noise effect, which is below 1.6%.

The false count is 0 cm^{-3} for GRIMM 11-D (tested with a zero filter at the inlet of the OPC). We can see that the CE of 11-D is very stable for concentrations from 1228 cm^{-3} to 0.5 cm^{-3}. Thus the CE of 11-D at low particle concentration of 0.5 cm^{-3} should be very close to that at high concentration of ~1000 cm^{-3}, with potentially small variation due to measurement noise (which is smaller than the expanded calibration uncertainty). The small deviation in the CE calibrated by NMC and NMIJ system at 0.5 μm (E_n <1) is a strong evidence of the equivalence of our PNC standards, although the concentration levels are different between the two setups.

In future work, we plan to use the particle concentration dilution method [77] to further check the CE's variation for particle concentrations from 1000 to 1 cm^{-3} using the GRIMM 11-D as a different approach. The basic idea is that lower particle concentration is generated by diluting a particle stream with known concentration of ~1000 cm^{-3}, which can be used to calibrate an OPC at low concentration of 1 or 10 cm^{-3}. This can help to establish the traceability in OPC calibration for concentration range from 1000 to 1 cm^{-3} using the FCAE-based PNC standard. This new method can also be used to further verify the equivalence of the FCAE-based PNC standards and IAG based standards via a different approach.

6. Conclusion

Results of the first inter-NMI comparison on the CE of OPC (GRIMM 11-D) at 0.3 μm and 0.5 μm have been reported for high concentration up to ~1000 cm^{-3}. The transfer standard has been calibrated by the primary PNC standard of NMC and NMIJ, using monodisperse PSL particles and LM particles. The CE of the OPC vs. a range of particle concentrations from ~200 to ~1500 cm^{-3} with particle size at 0.3 μm has been evaluated using a reference CPC to check the stability of the CE and potential coincidence error effect. We have selected a particle concentration at ~1000 cm^{-3} for calibration by the FCAE which is free from coincidence error effect on the CE. The setup and measurement uncertainty of the primary PNC standards have been described.

The CEs of the OPC around 0.3 μm measured by NMC and NMIJ agree with each other within the measurement uncertainties (E_n < 1), which shows the equivalence of the PNC standards of both institutes at high particle concentration up to 1000 cm^{-3}. The small deviation in the CE calibrated by NMC and NMIJ system at 0.5 μm (E_n < 1) is a strong evidence of the equivalence of our PNC standards, although it was compared at different concentration levels. This is based on the analysis on the CE's small variation (<1.6%) at decreasing concentration levels from 1228 to 0.5 cm^{-3} , which basically comes from measurement noise and is good evidence for the stability of the CE within this concentration range. The CE of the OPC around 0.3 and 0.5 μm measured by two institutes in this comparison have achieved an agreement within 1.5%, which is better than previous inter-NMI comparisons. In future work, we plan to develop a particle concentration dilution method to extend the OPC calibration concentration to 1 cm^{-3} using FCAE. This new method can be used to further verify the equivalence of the FCAE-based PNC standards and IAG based standards as a different approach.

Reference

[1] F. Cobo, D. Grela, A. Conchal, Airborne particle monitoring in clean room environments for stem cell cultures, Biotechnol. J. 3 (2008) 43–52.

[2] P. Görner, X. Simon, D. Bémer, G. Lidén, Workplace aerosol mass concentration measurement using optical particle counters, J. Environ. Monit. 14 (2012) 420–428.

[3] A. Tittarelli, A. Borgini, M. Bertoldi, E. De Saeger, A. Ruprecht, R. Stefanoni, G. Tagliabue, P. Contiero, P. Crosignani, Estimation of particle mass concentration in ambient air using a particle counter, Atmos. Environ. 42 (2008) 8543–8548.

[4] A. Konda, A. Prakash, G.A. Moss, M. Schmoldt, G.D. Grant, S. Guha, Aerosol Filtration Efficiency of Common Fabrics Used in Respiratory Cloth Masks, ACS Nano. 14 (2020) 6339–6347.

[5] W.G. Lindsley, W.P. King, R.E. Thewlis, J.S. Reynolds, K. Panday, G. Cao, J. V. Szalajda, Dispersion and exposure to a cough-generated aerosol in a simulated medical examination room, J. Occup. Environ. Hyg. 9 (2012) 681–690.

[6] W.W. Szymanski, Y.H. Cheng, C.J. Tsai, Filter efficiency measurements with optical particle counters - limitations and error sources, Sep. Sci. Technol. 33 (1998) 1225–1240.

[7] A. Dinoi, A. Donateo, M. Conte, M. Conte, F. Belosi, Comparison of atmospheric particle concentration measurements using different optical detectors: Potentiality and limits for air quality applications, Measurement. 106 (2017) 274–282.

[8] P. Abdolghader, C. Brochot, F. Haghighat, A. Bahloul, Procedure to measure the penetration of one mechanical filter for nanoparticles – Validation by comparison, Measurement. 147 (2019) 106840.

[9] B.T. Chen, Y.S. Cheng, H.C. Yeh, Experimental responses of two optical particle counters, J. Aerosol Sci. 15 (1984) 457–464.

[10] A. Czitrovszky, Applications of Optical Methods for Micrometer and Submicrometer Particle Measurements, in: Aerosols - Sci. Technol., Wiley-VCH, 2010: pp. 203–239.

[11] W.W. Szymanski, B.Y.H. Liu, On the Sizing Accuracy of Laser Optical Particle Counters, Part. Part. Syst. Charact. 3 (1986) 1–7.

[12] W.W. Szymanski, A. Nagy, A. Czitrovszky, Optical particle spectrometry-Problems and prospects, J. Quant. Spectrosc. Radiat. Transf. 110 (2009) 918–929.

[13] B.Y.H. Liu, W.W. Szymanski, K.H. Ahn, On aerosol size distribution measurement by laser and white light optical particle counters, J. Environ. Sci. 28 (1985) 19–24.

[14] H. Zhou, Y. Song, X. Pan, D. Li, Airborne particles detection and sizing at single particle level by a

novel electrical current pulse sensor, Measurement. 92 (2016) 58–62.

[15] D. Scaccabarozzi, B. Saggin, C. Pagliara, M. Magni, M. Tarabini, F. Esposito, C. Molfese, F. Cozzolino, F. Cortecchia, G. Dolnikov, I. Kuznetsov, A. Lyash, A. Zakharov, MicroMED, design of a particle analyzer for Mars, Measurement. 122 (2018) 466–472.

[16] M. Carminati, G. Ferrari, M. Sampietro, Emerging miniaturized technologies for airborne particulate matter pervasive monitoring, Measurement. 101 (2017) 250–256.

[17] D. Bemer, J.F. Fabries, A. Renoux, Calculation of the theoretical response of an optical particle counter and its practical usefulness, J. Aerosol Sci. 21 (1990) 689–700.

[18] J. Schlatter, A primary standard for particle number concentrations, in: Proc. 12th Int. Metrol. Congr., 2005.

[19] J. Schlatter, Measurement of particles in aerosols - Challenge and solutions, Chim. Int. J. Chem. 63 (2009) 665–669.

[20] W.C. Hinds, G. Kraske, Performance of PMS model LAS-X optical particle counter, J. Aerosol Sci. 17 (1986) 67–72.

[21] H.Y. Wen, G. Kasper, Counting efficiencies of six commercial particle counters, J. Aerosol Sci. (1986) 947–961.

[22] M. Heim, B.J. Mullins, H. Umhauer, G. Kasper, Performance evaluation of three optical particle counters with an efficient "multimodal" calibration method, J. Aerosol Sci. (2008) 1019–1031.

[23] A. van der Meulen, A. Plomp, F. Oeseburg, E. Buringh, R.M. van Aalst, W. Hoevers, Intercomparison of optical particle counters under conditions of normal operation, Atmos. Environ. 14 (1980) 495–499.

[24] J. Mäkynen, J. Hakulinen, T. Kivistö, M. Lehtimäki, Optical particle counters: Response, resolution and counting efficiency, J. Aerosol Sci. 13 (1982) 529–535.

[25] J. Burkart, G. Steiner, G. Reischl, H. Moshammer, M. Neuberger, R. Hitzenberger, Characterizing the performance of two optical particle counters (Grimm OPC1.108 and OPC1.109) under urban aerosol conditions, J. Aerosol Sci. 41 (2010) 953–962.

[26] N. Sang-Nourpour, J.S. Olfert, Calibration of optical particle counters with an aerodynamic aerosol classifier, J. Aerosol Sci. 138 (2019) 105452.

[27] ISO, ISO 21501-1:2009 - Determination of particle size distribution — Single particle light interaction methods — Part 1: Light scattering aerosol spectrometer, 2009.

[28] ISO, ISO 21501-4:2018 - Determination of particle size distribution — Single particle light interaction methods — Part 4: Light scattering airborne particle counter for clean spaces, 2018.

[29] K. Vasilatou, C. Wälchli, S. Koust, S. Horender, K. Iida, H. Sakurai, F. Schneider, J. Spielvogel, T.Y. Wu, K. Auderset, Calibration of optical particle size spectrometers against a primary standard: Counting efficiency profile of the TSI Model 3330 OPS and Grimm 11-D monitor in the particle size range from 300 nm to 10 μm, J. Aerosol Sci. 157 (2021) 105818.

[30] W. Winklmayr, G.P. Reischl, A.O. Lindner, A. Berner, A new electromobility spectrometer for the measurement of aerosol size distributions in the size range from 1 to 1000 nm, J. Aerosol Sci. 22 (1991) 289–296.

[31] G.P. Reischl, The relationship of input and output aerosol characteristics for an ideal differential mobility analyser particle standard, J. Aerosol Sci. 22 (1991) 297–312.

[32] R.A. Fletcher, G.W. Mulholland, M.R. Winchester, R.L. King, & D.B. Klinedinst, Calibration of a Condensation Particle Counter Using a NIST Traceable Method, Aerosol Sci. Technol. 43 (2009) 425–441.

[33] N. Takegawa, H. Sakurai, Laboratory evaluation of a TSI condensation particle counter (Model 3771) under airborne measurement conditions, Aerosol Sci. Technol. 45 (2011) 272–283. https://doi.org/10.1080/02786826.2010.532839.

[34] J. Yli-Ojanperä, H. Sakurai, K. Iida, J.M. Mkel, K. Ehara, J. Keskinen, Comparison of three particle number concentration calibration standards through calibration of a single CPC in a wide particle size range, Aerosol Sci. Technol. (2012) 1163–1173.

[35] B. Giechaskiel, X. Wang, H.G. Horn, J. Spielvogel, C. Gerhart, J. Southgate, L. Jing, M. Kasper, Y. Drossinos, A. Krasenbrink, Calibration of condensation particle counters for legislated vehicle

number emission measurements, Aerosol Sci. Technol. 43 (2009) 1164–1173.

[36] X. Wang, R. Caldow, G.J. Sem, N. Hama, H. Sakurai, Evaluation of a condensation particle counter for vehicle emission measurement: Experimental procedure and effects of calibration aerosol material, J. Aerosol Sci. (2010).

[37] J. Schlatter, Final Report of EURAMET Project 1027, Comparison of nanoparticle number concentration and size distribution, 2009. www.euramet.org.

[38] P. Quincey, D. Sarantaridis, T. Tuch, J. Yli-Ojanperä, EURAMET Comparison 1282 Final Report: Comparison of condensation particle counters., 2014.

[39] R. Högström, P. Quincey, D. Sarantaridis, F. Lönd, A. Nowak, F. Riccobono, T. Tuch, H. Sakurai, M. Owen, M. Heinonen, J. Keskinen, J. Yli-Ojanperä, First comprehensive inter-comparison of aerosol electrometers for particle sizes up to 200nm and concentration range 1000cm-3 to 17 000cm -3, Metrologia. 51 (2014) 293–303.

[40] K. Ehara, H. Sakurai, Metrology of airborne and liquid-borne nanoparticles: Current status and future needs, Metrologia. 47 (2010) S83.

[41] J. Yli-Ojanperä, J.M. Mäkelä, M. Marjamäki, A. Rostedt, J. Keskinen, Towards traceable particle number concentration standard: Single charged aerosol reference (SCAR), J. Aerosol Sci. (2010).

[42] R. Högström, J. Yli-Ojanperä, A. Rostedt, I. Iisakka, J.M. Mäkelä, M. Heinonen, J. Keskinen, Validating the single charged aerosol reference (SCAR) as a traceable particle number concentration standard for 10 nm to 500 nm aerosol particles, Metrologia. (2011).

[43] K. Vasilatou, K. Dirscherl, K. Iida, H. Sakurai, S. Horender, K. Auderset, Calibration of optical particle counters: First comprehensive inter-comparison for particle sizes up to 5 μm and number concentrations up to 2 cm-3, Metrologia. (2020) 025005.

[44] N.A. Fuchs, On the stationary charge distribution on aerosol particles in a bipolar ionic atmosphere, Geofis. Pura e Appl. 56 (1963) 185–193.

[45] W.A. Hoppel, G.M. Frick, Ion—aerosol attachment coefficients and the steady-state charge distribution on aerosols in a bipolar ion environment, Aerosol Sci. Technol. 5 (1986) 1–21.

[46] B.Y.H. Liu, D.Y.H. Pui, Equilibrium bipolar charge distribution of aerosols, J. Colloid Interface Sci. 49 (1974) 305–312.

[47] A. Wiedensohler, An approximation of the bipolar charge distribution for particles in the submicron size range, J. Aerosol Sci. 19 (1988) 387–389.

[48] E.O. Knutson, K.T. Whitby, Aerosol classification by electric mobility: apparatus, theory, and applications, J. Aerosol Sci. 6 (1975) 443–451.

[49] Y. Kousaka, K. Okuyama, M. Adachi, Determination of particle size distribution of ultra-fine aerosols using a differential mobility analyzer, Aerosol Sci. Technol. 4 (1985) 209–225.

[50] M.R. Stolzenburg, A review of transfer theory and characterization of measured performance for differential mobility analyzers, Aerosol Sci. Technol. 52 (2018) 1194–1218.

[51] B.Y.H. Liu, D.Y.H. Pui, A submicron aerosol standard and the primary, absolute calibration of the condensation nuclei counter, J. Colloid Interface Sci. 47 (1974) 155–171.

[52] H. Sakurai, K. Ehara, Evaluation of uncertainties in femtoampere current measurement for the number concentration standard of aerosol nanoparticles, Meas. Sci. Technol. 22 (2011) 024009.

[53] K. Pihlava, J. Keskinen, J. Yli-Ojanperä, Improving the signal-to-noise ratio of Faraday cup aerosol electrometer based aerosol instrument calibrations, Aerosol Sci. Technol. 50 (2016) 373–379.

[54] A. Järvinen, J. Keskinen, J. Yli-Ojanperä, Extending the Faraday cup aerosol electrometer based calibration method up to 5 μm, Aerosol Sci. Technol. 52 (2018) 828–840.

[55] D.G. Jarrett, M.C. Owen, Traceability for aerosol electrometer in the fA range, in: 19th IMEKO TC4 Symp. - Meas. Electr. Quant., 2013: pp. 270–274.

[56] G.D. Willenberg, H.N. Tauscher, P. Warnecke, A traceable precision current source for currents between 100 aA and 10 pA, IEEE Trans. Instrum. Meas. 52 (2003) 436–439.

[57] JCGM 100:2008, Evaluation of measurement data - Guide to the expression of uncertainty in measurement, Joint Committees for Guides in Metrology, 2008.

[58] ISO 27891:2015, Aerosol Particle Number Concentration—Calibration of Condensation Particle

Counters, International Organization for Standardization, 2015.

[59] K. Iida, H. Sakurai, K. Saito, K. Ehara, Inkjet aerosol generator as monodisperse particle number standard, Aerosol Sci. Technol. 48 (2014) 789–802.

[60] K. Iida, H. Sakurai, Counting efficiency evaluation of optical particle counters in micrometer range by using an inkjet aerosol generator, Aerosol Sci. Technol. (2018) 1156–1166.

[61] T. Minakami, T. Hosokawa, K. Kondo, K. Iida, K. Ehara, H. Sakurai, Evaluation of Counting Efficiencies for Optical Particle Counters by using Inkjet Aerosol Generator, Earozoru Kenkyu. 32 (2017) 29–36.

[62] L.H. Princen, W.F. Kwolek, Coincidence corrections for particle size determinations with the Coulter counter, Rev. Sci. Instrum. 36 (1965) 646–653.

[63] J.F. Pisani, G.H. Thomson, Coincidence errors in automatic particle counters, J. Phys. E. 4 (1971) 359–361.

[64] R. Jaenicke, The optical particle counter: Cross-sensitivity and coincidence, J. Aerosol Sci. 3 (1972) 95–111.

[65] J. Raasch, H. Umhauer, Der Koinzidenzfehler bei der Streulicht-Partikelgrößen-Zählanalyse, Fortschrittberichte Der VDI-Zeitschriften, R. 3, Nr. 95. (1984).

[66] J. Raasch, H. Umhauer, Errors in the Determination of Particle Size Distributions Caused by coincidences in optical particle counters, Part. Part. Syst. Charact. 1 (1984) 53–58.

[67] K.T. Whitby, K. Willeke, Single Particle Optical Counters: Principles and Field Use, in: Lundgren, D.A., Lippmann, M., Harris, F.S., Clark, W.E., Marlow, W.H., Durham, M.D. (Eds.), Aerosol Meas., University Presses of Florida, Gainesville, FL, 1979: pp. 145–182.

[68] J. Gebhart, Funktionsweise und Eigenschaften optischer Partikelzähler, Tech. Mess. 56 (1989) 192–203. https://doi.org/10.1524/teme.1989.56.jg.192.

[69] S. V Hering, M.R. Stolzenburg, F.R. Quant, D.R. Oberreit, P.B. Keady, A Laminar-Flow, Water-Based Condensation Particle Counter (WCPC), Aerosol Sci. Technol. 39 (2005) 659–672.

[70] C.M. Sorensen, J. Gebhart, T.J. O'Hern, D.J. Rader, Optical Measurement Techniques: Fundamentals and Applications, Aerosol Meas. Princ. Tech. Appl. Third Ed. (2011) 269–312.

[71] J. Gebhart, Optical Direct-Reading Techniques: Light Intensity Systems, P. A. Baron K. Willeke, Eds., Aerosol Meas. (1993) 313–344.

[72] B. Sachweh, H. Umhauer, F. Ebert, H. Büttner, R. Friehmelt, In situ optical particle counter with improved coincidence error correction for number concentrations up to 107 particles cm−3, J. Aerosol Sci. 29 (1998) 1075–1086.

[73] J.H. Bushill, W.B. Wright, C.H.F. Fuller, A. V. Bell, The crystallisation of lactose with particular reference to its occurrence in milk powder, J. Sci. Food Agric. 16 (1965) 622–628.

[74] E.J. Davis, P. Ravindran, Single particle light scattering measurements using the electrodynamic balance, Aerosol Sci. Technol. 1 (1982) 337–350.

[75] R.G. Knollenberg, The measurement of latex particle sizes using scattering ratios in the rayleigh scattering size range, J. Aerosol Sci. 20 (1989) 331–345.

[76] ISO/IEC, ISO/IEC 17043, Conformity assessment - General requirements for proficiency testing, (2010).

[77] M. Owen, G. Mulholland, W. Guthrie, Condensation Particle Counter Proportionality Calibration from 1 Particle·cm −3 to 10 4 Particles·cm −3, Aerosol Sci. Technol. 46 (2012) 444–450.